SANTA CRUZ BIOTECHNOLOGY, INC.

HAT1 (H-7): sc-390562

SANTA CRUZ BIOTECHNOLOGY

The Power to Question

BACKGROUND

In the intact cell, DNA closely associates with histones and other nuclear proteins to form chromatin. The remodeling of chromatin is believed to be a critical component of transcriptional regulation and a major source of this remodeling is brought about by the acetylation of nucleosomal histones. Acetylation of lysine residues in the amino-terminal tail domain of histone results in an allosteric change in the nucleosomal conformation and an increased accessibility to transcription factors by DNA. Conversely, the deacetylation of histones is associated with transcriptional silencing. Several mammalian proteins have been identified as nuclear histone acetylases, including GCN5, PCAF (p300/CBP-associated factor), p300/CBP, HAT1 and the TFIID subunit TAF II p250. Mammalian HDAC1 (also designated HD1), HDAC2 (also designated RPD3) and HDAC3-6 have been identified as histone deacetylases.

CHROMOSOMAL LOCATION

Genetic locus: HAT1 (human) mapping to 2q31.1; Hat1 (mouse) mapping to 2 C2.

SOURCE

HAT1 (H-7) is a mouse monoclonal antibody raised against amino acids 1-300 mapping raised against amino acids 1-300 of HAT1 of human origin.

PRODUCT

Each vial contains 200 µg IgG_1 kappa light chain in 1.0 ml of PBS with < 0.1% sodium azide and 0.1% gelatin.

HAT1 (H-7) is available conjugated to agarose (sc-390562 AC), 500 µg/0.25 ml agarose in 1 ml, for IP; to HRP (sc-390562 HRP), 200 µg/ml, for WB, IHC(P) and ELISA; to either phycoerythrin (sc-390562 PE), fluorescein (sc-390562 FITC), Alexa Fluor® 488 (sc-390562 AF488), Alexa Fluor® 546 (sc-390562 AF546), Alexa Fluor® 594 (sc-390562 AF594) or Alexa Fluor® 647 (sc-390562 AF647), 200 µg/ml, for WB (RGB), IF, IHC(P) and FCM; and to either Alexa Fluor® 680 (sc-390562 AF680) or Alexa Fluor® 790 (sc-390562 AF790), 200 µg/ml, for Near-Infrared (NIR) WB, IF and FCM.

APPLICATIONS

HAT1 (H-7) is recommended for detection of HAT1 of mouse, rat and human origin by Western Blotting (starting dilution 1:100, dilution range 1:100-1:1000), immunoprecipitation [1-2 µg per 100-500 µg of total protein (1 ml of cell lysate)], immunofluorescence (starting dilution 1:50, dilution range 1:50-1:500), immunohistochemistry (including paraffin-embedded sections) (starting dilution 1:50, dilution range 1:50-1:500) and solid phase ELISA (starting dilution 1:30, dilution range 1:30-1:3000).

Suitable for use as control antibody for HAT1 siRNA (h): sc-37948, HAT1 siRNA (m): sc-145898, HAT1 shRNA Plasmid (h): sc-37948-SH, HAT1 shRNA Plasmid (m): sc-145898-SH, HAT1 shRNA (h) Lentiviral Particles: sc-37948-V and HAT1 shRNA (m) Lentiviral Particles: sc-145898-V.

Molecular Weight of HAT1: 42 kDa.

Positive Controls: F9 cell lysate: sc-2245, MCF7 whole cell lysate: sc-2206 or Jurkat whole cell lysate: sc-2204.

STORAGE

Store at 4° C, **DO NOT FREEZE**. Stable for one year from the date of shipment. Non-hazardous. No MSDS required.

DATA

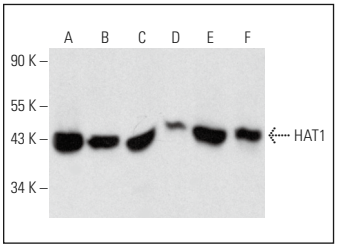

HAT1 (H-7): sc-390562. Western blot analysis of HAT1 expression in Jurkat (**A**), MCF7 (**B**), F9 (**C**), RAW 264.7 (**D**), RBL-1 (**E**) and C6 (**F**) whole cell lysates.

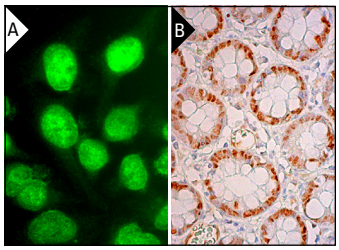

HAT1 (H-7): sc-390562. Immunofluorescence staining of methanol-fixed HeLa cells showing nuclear localization (**A**). Immunoperoxidase staining of formalin fixed, paraffin-embedded human colon tissue showing nuclear staining of glandular cells (**B**).

SELECT PRODUCT CITATIONS

1. Maudet, A., et al. 2013. HIV-1 Vpr induces the degradation of ZIP and sZIP, adaptors of the NuRD chromatin remodeling complex, by hijacking DCAF1/VprBP. PLoS ONE 8: e77320.
2. Xue, L., et al. 2014. RNAi screening identifies HAT1 as a potential drug target in esophageal squamous cell carcinoma. Int. J. Clin. Exp. Pathol. 7: 3898-3907.
3. Strub, T., et al. 2018. SIRT6 haploinsufficiency induces $BRAF^{V600E}$ melanoma cell resistance to MAPK inhibitors via IGF signalling. Nat. Commun. 9: 3440.
4. Sun, W., et al. 2019. Monitoring structural modulation of redox-sensitive proteins in cells with MS-CETSA. Redox Biol. 24: 101168.
5. Liu, N., et al. 2020. The cross-talk between methylation and phosphorylation in lymphoid-specific helicase drives cancer stem-like properties. Signal Transduct. Target. Ther. 5: 197.
6. Yu, X.H., et al. 2020. LncRNA kcnq1ot1 promotes lipid accumulation and accelerates atherosclerosis via functioning as a ceRNA through the miR-452-3p/HDAC3/ABCA1 axis. Cell Death Dis. 11: 1043.
7. Baas, R., et al. 2021. Proteomic analysis identifies novel binding partners of BAP1. PLoS ONE 16: e0257688.
8. Gandhi, S., et al. 2022. Mitotic H3K9ac is controlled by phase-specific activity of HDAC2, HDAC3, and SIRT1. Life Sci. Alliance 5: e202201433.
9. Terada, C.I., et al. 2022. Histopathological and epigenetic changes in myocardium associated with cancer therapy-related cardiac dysfunction. ESC Heart Fail. 9: 3031-3043.

RESEARCH USE

For research use only, not for use in diagnostic procedures.